NASA TECHNICAL NOTE

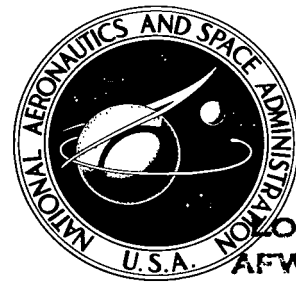

NASA TN D-8217

TIME-ASYMPTOTIC SOLUTIONS OF THE NAVIER-STOKES EQUATIONS FOR FREE SHEAR FLOWS USING AN ALTERNATING-DIRECTION IMPLICIT METHOD

David H. Rudy and Dana J. Morris

Langley Research Center
Hampton, Va. 23665

NATIONAL AERONAUTICS AND SPACE ADMINISTRATION • WASHINGTON, D. C. • OCTOBER 1976

1. Report No.	2. Government Accession No.	3. Recipient's Catalog No.
NASA TN D-8217		

4. Title and Subtitle	5. Report Date
TIME-ASYMPTOTIC SOLUTIONS OF THE NAVIER-STOKES EQUATIONS FOR FREE SHEAR FLOWS USING AN ALTERNATING-DIRECTION IMPLICIT METHOD	October 1976
	6. Performing Organization Code

7. Author(s)	8. Performing Organization Report No.
David H. Rudy and Dana J. Morris	L-10669
	10. Work Unit No.
	505-06-11-03

9. Performing Organization Name and Address	11. Contract or Grant No.
NASA Langley Research Center Hampton, VA 23665	
	13. Type of Report and Period Covered
	Technical Note

12. Sponsoring Agency Name and Address	14. Sponsoring Agency Code
National Aeronautics and Space Administration Washington, DC 20546	

15. Supplementary Notes

16. Abstract

An uncoupled time-asymptotic alternating-direction implicit method for solving the Navier-Stokes equations was tested on two laminar parallel mixing flows. A constant total temperature was assumed in order to eliminate the need to solve the full energy equation; consequently, static temperature was evaluated by using an algebraic relationship. For the mixing of two supersonic streams at a Reynolds number of 10^3, converged solutions were obtained for a time step 5 times the maximum allowable size for an explicit method. The solution diverged for a time step 10 times the explicit limit. Improved convergence was obtained when upwind differencing was used for convective terms. Larger time steps were not possible with either upwind differencing or the diagonally dominant scheme of Khosla and Rubin. Artificial viscosity was added to the continuity equation in order to eliminate divergence for the mixing of a subsonic stream with a supersonic stream at a Reynolds number of 10^3.

17. Key Words (Suggested by Author(s))	18. Distribution Statement
Navier-Stokes equations Compressible flow Finite-difference method	Unclassified – Unlimited Subject Category 34

19. Security Classif. (of this report)	20. Security Classif. (of this page)	21. No. of Pages	22. Price*
Unclassified	Unclassified	37	$3.75

*For sale by the National Technical Information Service, Springfield, Virginia 22161

TIME-ASYMPTOTIC SOLUTIONS OF THE NAVIER-STOKES EQUATIONS FOR FREE SHEAR FLOWS USING AN ALTERNATING-DIRECTION IMPLICIT METHOD

David H. Rudy and Dana J. Morris
Langley Research Center

SUMMARY

An uncoupled time-asymptotic alternating-direction implicit method for solving the Navier-Stokes equations was tested on two laminar parallel mixing flows. A constant total temperature was assumed in order to eliminate the need to solve the full energy equation; consequently, static temperature was evaluated by using an algebraic relationship. For the mixing of two supersonic streams at a Reynolds number of 10^3, converged solutions were obtained for a time step 5 times the maximum allowable size for an explicit method. The solution diverged for a time step 10 times the explicit limit. Improved convergence was obtained when upwind differencing was used for convective terms. Larger time steps were not possible with either upwind differencing or the diagonally dominant scheme of Khosla and Rubin. Artificial viscosity was added to the continuity equation in order to eliminate divergence for the mixing of a subsonic stream with a supersonic stream at a Reynolds number of 10^3.

INTRODUCTION

This report presents the results of an investigation using an uncoupled alternating-direction implicit (ADI) finite-difference technique to obtain steady-state solutions for two-dimensional, high Reynolds number, compressible free shear flows by using a time-asymptotic approach. Preliminary results from this study are presented in reference 1.

The review papers of Peyret and Viviand (ref. 2) and Taylor (ref. 3) summarize the published finite-difference solutions of the viscous compressible time-dependent Navier-Stokes equations. Most of the published solutions have used explicit differencing schemes. Although they are conceptually less complex and thus more easily coded than implicit methods, explicit finite-difference methods are restricted to small time steps relative to the spatial grid size for numerical stability. Consequently, explicit methods generally require a large total computation time to reach a steady-state flow condition. On the other hand, most implicit methods are found to be unconditionally stable in linearized stability analyses for model equations similar to the Navier-Stokes equations. Therefore, it is

expected that implicit methods will allow larger time steps than explicit methods when applied to the Navier-Stokes equations.

The ADI technique developed by Peaceman and Rachford (ref. 4) and Douglas (ref. 5) was used in the present study. This ADI method is a two-step procedure requiring reduction of tridiagonal matrices for which an efficient solution algorithm, the Thomas algorithm (ref. 6), exists. The method was originally applied to the two-dimensional heat conduction equation in reference 4 and was later applied to a system of hyperbolic equations by Gourlay and Mitchell (ref. 7). For both of these model problems, the ADI method was shown to possess unconditional stability. Roache (ref. 8) states that ADI methods are currently the most popular approach to computing incompressible viscous Navier-Stokes flows. He notes that although these methods have not been found to be unconditionally stable in practice, the somewhat larger time steps obtainable have resulted in faster overall computation times (by a factor of 2 or more) than explicit methods for such flows.

The ADI method has been applied to the time-dependent compressible Navier-Stokes equations in only a few papers. In 1966, Polezhaev (ref. 9), for example, used an ADI method to obtain solutions for a two-dimensional natural convection problem. His uncoupled ADI procedure removed the diffusion time-step limitation; however, he found that a sufficient condition for stability limited the time step to the usual maximum explicit value. In 1973, Briley and McDonald (ref. 10) presented a coupled ADI method in which nonlinearities at the implicit time level were linearized by using a Taylor's series expansion about the known time level. The resulting system of linear difference equations was solved simultaneously by using a Douglas-Gunn (ref. 11) ADI approach. The method was found to be stable for very large Courant numbers $\left(N_{Co} = 1 \text{ corresponds to the Courant-Freidrichs-Lewy condition}\right)$ in the calculation of three-dimensional subsonic flow in a straight duct with a rectangular cross section. For a flow with a Mach number of 0.044 and a Reynolds number of 60, stable solutions were obtained for Courant numbers up to 1250. For a Mach number of 0.5 and a Reynolds number of 600, the time step was gradually increased as the solution progressed; this gave an average Courant number of 73. Thus, the maximum Courant number decreased with increasing Reynolds number, perhaps because of diagonal dominance problems in the coefficient matrix as suggested in reference 10. The computational effort per time step was reported to be twice that of most explicit methods. Baum and Ndefo (ref. 12) have also published an implicit method based on the Peaceman-Rachford procedure. This method iteratively solves coupled nonlinear difference equations by using a quasi-linearization technique. Reference 12 does not include results from solutions of the compressible Navier-Stokes equations. However, in reference 13 the method has been applied to the laminar hypersonic near wake of a sharp cone.

The ADI method investigated in the present paper is an uncoupled procedure which is applied to the mixing of two parallel streams. The results of reference 1 for the mixing of two supersonic streams have been improved for central differencing and extended to include computations with two other forms of differencing which give unconditional diagonal dominance in the coefficient matrices. In addition, results are presented for the mixing of a subsonic stream with a supersonic stream.

SYMBOLS

c	speed of sound
H	enthalpy
L	reference length ($\bar{L}$ = 2.54 cm)
M	Mach number
N_{Co}	Courant number, $\dfrac{\Delta t}{\dfrac{\Delta x}{\lvert u\rvert + \lvert v\rvert + \sqrt{2}c}}$
N_{Re}	Reynolds number, $\dfrac{\bar{\rho}_s \bar{u}_{ref} \bar{L}}{\bar{\mu}_s}$
p	pressure
R	gas constant
S	$= 198.6/\overline{T}_s$
T	temperature
t	time
u	streamwise velocity (x-direction)
u_{ref}	reference velocity, $\sqrt{2\overline{H}_s}$
u_1	free-stream velocity on low-velocity side of mixing region

u_2	free-stream velocity on high-velocity side of mixing region
v	normal velocity (y-direction)
x,y	coordinates in streamwise and normal directions, respectively
α	artificial diffusion coefficient
γ	ratio of specific heats
μ	molecular viscosity
ρ	density
x_{max}, y_{max}	maximum values of x and y, respectively, in solution domain

Subscripts:

i,j	index denoting grid-point spatial location
s	stagnation condition
t,x,y	derivative with respect to time, x-direction, and y-direction, respectively

Superscripts:

n,*	index denoting time level

Abbreviations:

ADI	alternating-direction implicit
IC	initial condition

A bar over a symbol denotes a dimensional quantity.

GOVERNING EQUATIONS

The nonconservative form of the governing partial differential equations was used in the present investigation. These equations are written as follows:

Continuity

$$\rho_t + \rho v_y + \rho u_x + v\rho_y + u\rho_x = 0 \tag{1}$$

x-momentum

$$\rho u_t + \rho v u_y + \rho u u_x = -p_x + \frac{4}{3N_{Re}}\left(\mu u_x\right)_x - \frac{2}{3N_{Re}}\left(\mu v_y\right)_x + \frac{1}{N_{Re}}\left[\mu\left(u_y + v_x\right)\right]_y \tag{2}$$

y-momentum

$$\rho v_t + \rho v v_y + \rho u v_x = -p_y + \frac{4}{3N_{Re}}\left(\mu v_y\right)_y - \frac{2}{3N_{Re}}\left(\mu u_x\right)_y + \frac{1}{N_{Re}}\left[\mu\left(u_y + v_x\right)\right]_x \tag{3}$$

These equations are nondimensionalized with respect to a reference length and stagnation flow conditions, that is,

$$\rho = \frac{\bar{\rho}}{\bar{\rho}_s} \qquad p = \frac{\bar{p}}{2\bar{\rho}_s \bar{H}_s}$$

$$T = \frac{\bar{T}}{\bar{T}_s} \qquad x = \frac{\bar{x}}{\bar{L}}$$

$$\bar{u}_{ref} = \sqrt{2\bar{H}_s} \qquad y = \frac{\bar{y}}{\bar{L}}$$

$$u = \frac{\bar{u}}{\sqrt{2\bar{H}_s}} = \frac{\bar{u}}{\bar{u}_{ref}} \qquad N_{Re} = \frac{\bar{\rho}_s \bar{u}_{ref} \bar{L}}{\bar{\mu}_s}$$

$$v = \frac{\bar{v}}{\sqrt{2\bar{H}_s}} = \frac{\bar{v}}{\bar{u}_{ref}} \qquad \mu = \frac{\bar{\mu}}{\bar{\mu}_s}$$

$$t = \frac{\bar{t}\bar{u}_{ref}}{\bar{L}}$$

The pressure was evaluated by means of the perfect gas equation of state

$$p = \rho R T \tag{4}$$

where $R = \frac{\gamma - 1}{2\gamma}$. Air ($\gamma = 1.4$) was the test fluid. Only laminar (molecular) viscous effects were considered, with the Sutherland formula being used to express the viscosity as a function of temperature as follows:

$$\mu = T^{3/2} \frac{1 + S}{T + S} \tag{5}$$

Calculations for a Mach 3 jet into still air with the quasi-parallel code of Oh (ref. 14), which includes the energy equation, showed that there was less than a 5-percent variation in the total enthalpy throughout the mixing region from the constant value assumed in other calculations. For the conditions of case 1 (supersonic-supersonic parallel mixing), the calculations of Oh showed less than a 1-percent variation in total enthalpy. This small variation had a negligible effect on the other flow parameters. Thus, to simplify the system of governing equations and to reduce required machine storage, a constant total temperature of 294 K (530° R) was assumed. Therefore, the static temperature was evaluated by use of the algebraic relationship

$$T = 1 - \left(u^2 + v^2\right) \tag{6}$$

which eliminated the need for solving the complete energy equation. Constant static pressure was assumed in order to generate initial values of density by using equations (4) and (6) along with the given initial velocities. The linearized version of equations (1) to (6) with the viscous terms neglected has been shown by Gottlieb and Gustafsson (ref. 15) to be well-posed for the initial value problem. Polezhaev (ref. 9) considered the nonconservative form of the momentum and energy equations but used the conservative form of the continuity equation. Briley and McDonald (ref. 10) used the conservative form except for the energy equation in their coupled procedure.

DESCRIPTION OF NUMERICAL TECHNIQUE

Solution Procedure

In the ADI procedure used in the present investigation, a sequential (uncoupled) solution of the finite-difference form of equations (1) to (3) is obtained for each interior row of grid points during the first one-half time step (horizontal sweep) and for each interior column of grid points during the second one-half time step (vertical sweep). All spatial derivatives were approximated by centered (second-order) finite differences, and time derivatives were approximated by backward (first-order) differences. The nonlinear coefficients in the convective terms were lagged one-half time step. In addition, the pressure terms and cross-derivative terms were also treated explicitly in each sweep. At each

row or column the order of solution was as follows: (1) solve the x-momentum equation for u, (2) solve the y-momentum equation for v, and (3) solve the continuity equation for ρ. The temperature and viscosity were then updated for the entire flow field after each sweep. No iteration was performed at any time step during the calculation. After the horizontal sweep, the values of u, v, and ρ were updated for the two boundary rows of points (i.e., the first and last rows) according to the appropriate boundary conditions. Similarly, the first and last columns were updated after the vertical sweep. The solution was then marched in time, with steady state considered to be the asymptotic limit. This uncoupled technique was chosen to avoid the coding complexity and possible additional computing time associated with the block-tridiagonal structure of a fully coupled approach.

Finite-Difference Forms of Equations

x-momentum equation.- To illustrate the present ADI procedure, the finite-difference form of the x-momentum equation is shown. For the horizontal sweep, from time level n to an intermediate time denoted by *, with a uniform spatial grid,

$$\rho_{i,j}^{n}\left(\frac{u_{i,j}^{*}-u_{i,j}^{n}}{\Delta t/2}\right)+\rho_{i,j}^{n}v_{i,j}^{n}\left(\frac{u_{i,j+1}^{n}-u_{i,j-1}^{n}}{2\,\Delta y}\right)+\rho_{i,j}^{n}u_{i,j}^{n}\left(\frac{u_{i+1,j}^{*}-u_{i-1,j}^{*}}{2\,\Delta x}\right)=-\left(\frac{p_{i+1,j}^{n}-p_{i-1,j}^{n}}{2\,\Delta x}\right)$$

$$+\frac{1}{N_{Re}\,\Delta y}\left[\left(\frac{\mu_{i,j+1}^{n}+\mu_{i,j}^{n}}{2}\right)\left(\frac{u_{i,j+1}^{n}-u_{i,j}^{n}}{\Delta y}\right)-\left(\frac{\mu_{i,j}^{n}+\mu_{i,j-1}^{n}}{2}\right)\left(\frac{u_{i,j}^{n}-u_{i,j-1}^{n}}{\Delta y}\right)\right]$$

$$+\frac{1}{N_{Re}\,\Delta y}\left[\mu_{i,j+1}^{n}\left(\frac{v_{i+1,j+1}^{n}-v_{i-1,j+1}^{n}}{2\,\Delta x}\right)-\mu_{i,j-1}^{n}\left(\frac{v_{i+1,j-1}^{n}-v_{i-1,j-1}^{n}}{2\,\Delta x}\right)\right]$$

$$+\frac{4}{3N_{Re}\,\Delta x}\left[\left(\frac{\mu_{i+1,j}^{n}+\mu_{i,j}^{n}}{2}\right)\left(\frac{u_{i+1,j}^{*}-u_{i,j}^{*}}{\Delta x}\right)-\left(\frac{\mu_{i,j}^{n}+\mu_{i-1,j}^{n}}{2}\right)\left(\frac{u_{i,j}^{*}-u_{i-1,j}^{*}}{\Delta x}\right)\right]$$

$$-\frac{2}{3N_{Re}\,\Delta x}\left[\mu_{i+1,j}^{n}\left(\frac{v_{i+1,j+1}^{n}-v_{i+1,j-1}^{n}}{2\,\Delta y}\right)-\mu_{i-1,j}^{n}\left(\frac{v_{i-1,j+1}^{n}-v_{i-1,j-1}^{n}}{2\,\Delta y}\right)\right] \tag{7}$$

For the jth row, this equation has the tridiagonal matrix form

$$A_i u_{i-1,j}^{*}+B_i u_{i,j}^{*}+C_i u_{i+1,j}^{*}=D_i \tag{8}$$

where A_i, B_i, and C_i are matrix coefficients which are defined as follows:

$$A_i = \frac{-\rho^n_{i,j} u^n_{i,j}}{2\,\Delta x} - \frac{4}{3N_{Re}(\Delta x)^2}\left(\frac{\mu^n_{i,j} + \mu^n_{i-1,j}}{2}\right) \tag{9a}$$

$$B_i = \frac{2\rho^n_{i,j}}{\Delta t} + \frac{4}{3N_{Re}(\Delta x)^2}\left(\frac{\mu^n_{i,j} + \mu^n_{i-1,j}}{2}\right) + \frac{4}{3N_{Re}(\Delta x)^2}\left(\frac{\mu^n_{i+1,j} + \mu^n_{i,j}}{2}\right) \tag{9b}$$

$$C_i = \frac{\rho^n_{i,j} u^n_{i,j}}{2\,\Delta x} - \frac{4}{3N_{Re}(\Delta x)^2}\left(\frac{\mu^n_{i+1,j} + \mu^n_{i,j}}{2}\right) \tag{9c}$$

and D_i is a vector of quantities which are evaluated at time n. The unknowns are $u^*_{i-1,j}$, $u^*_{i,j}$, and $u^*_{i+1,j}$. Similarly, for the vertical sweep, from * to n + 1, the x-momentum equation in finite-difference form is given by

$$\rho^*_{i,j}\left(\frac{u^{n+1}_{i,j} - u^*_{i,j}}{\Delta t/2}\right) + \rho^*_{i,j} v^*_{i,j}\left(\frac{u^{n+1}_{i,j+1} - u^{n+1}_{i,j-1}}{2\,\Delta y}\right) + \rho^*_{i,j} u^*_{i,j}\left(\frac{u^*_{i+1,j} - u^*_{i-1,j}}{2\,\Delta x}\right) = -\left(\frac{p^*_{i+1,j} - p^*_{i-1,j}}{2\,\Delta x}\right)$$

$$+ \frac{1}{N_{Re}\,\Delta y}\left[\left(\frac{\mu^*_{i,j+1} + \mu^*_{i,j}}{2}\right)\left(\frac{u^{n+1}_{i,j+1} - u^{n+1}_{i,j}}{\Delta y}\right) - \left(\frac{\mu^*_{i,j} + \mu^*_{i,j-1}}{2}\right)\left(\frac{u^{n+1}_{i,j} - u^{n+1}_{i,j-1}}{\Delta y}\right)\right]$$

$$+ \frac{1}{N_{Re}\,\Delta y}\left[\mu^*_{i,j+1}\left(\frac{v^*_{i+1,j+1} - v^*_{i-1,j+1}}{2\,\Delta x}\right) - \mu^*_{i,j-1}\left(\frac{v^*_{i+1,j-1} - v^*_{i-1,j-1}}{2\,\Delta x}\right)\right]$$

$$+ \frac{4}{3N_{Re}\,\Delta x}\left[\left(\frac{\mu^*_{i+1,j} + \mu^*_{i,j}}{2}\right)\left(\frac{u^*_{i+1,j} - u^*_{i,j}}{\Delta x}\right) - \left(\frac{\mu^*_{i,j} + \mu^*_{i-1,j}}{2}\right)\left(\frac{u^*_{i,j} - u^*_{i-1,j}}{\Delta x}\right)\right]$$

$$- \frac{2}{3N_{Re}\,\Delta x}\left[\mu^*_{i+1,j}\left(\frac{v^*_{i+1,j+1} - v^*_{i+1,j-1}}{2\,\Delta y}\right) - \mu^*_{i-1,j}\left(\frac{v^*_{i-1,j+1} - v^*_{i-1,j-1}}{2\,\Delta y}\right)\right] \tag{10}$$

For the ith column, this equation has the tridiagonal matrix form

$$A_j u^{n+1}_{i,j-1} + B_j u^{n+1}_{i,j} + C_j u^{n+1}_{i,j+1} = D_j \tag{11}$$

where A_j, B_j, and C_j are matrix coefficients which are defined as follows:

$$A_j = \frac{-\rho^*_{i,j} v^*_{i,j}}{2\,\Delta y} - \frac{1}{N_{Re}(\Delta y)^2}\left(\frac{\mu^*_{i,j} + \mu^*_{i,j-1}}{2}\right) \tag{12a}$$

$$B_j = \frac{2\rho^*_{i,j}}{\Delta t} + \frac{1}{N_{Re}(\Delta y)^2}\left[\left(\frac{\mu^*_{i,j} + \mu^*_{i,j-1}}{2}\right) + \left(\frac{\mu^*_{i,j} + \mu^*_{i,j+1}}{2}\right)\right] \tag{12b}$$

$$C_j = \frac{\rho^*_{i,j} v^*_{i,j}}{2\,\Delta y} - \frac{1}{N_{Re}(\Delta y)^2}\left(\frac{\mu^*_{i,j} + \mu^*_{i,j+1}}{2}\right) \tag{12c}$$

and D_j is a vector of quantities which are evaluated at time $*$. The unknowns are $u^{n+1}_{i,j-1}$, $u^{n+1}_{i,j}$, and $u^{n+1}_{i,j+1}$. The accuracy of all the difference equations is $O(\Delta t, (\Delta x)^2, (\Delta y)^2)$. A more accurate transient solution was considered unnecessary since only the steady state was of interest.

y-momentum equation.- For the jth row during the horizontal sweep, the y-momentum equation is written

$$A_i v^*_{i-1,j} + B_i v^*_{i,j} + C_i v^*_{i+1,j} = D_i \tag{13}$$

where

$$A_i = \frac{-\rho^n_{i,j} u^*_{i,j}}{2\,\Delta x} - \frac{1}{N_{Re}(\Delta x)^2}\left(\frac{\mu^n_{i,j} + \mu^n_{i-1,j}}{2}\right) \tag{14a}$$

$$B_i = \frac{2\rho^n_{i,j}}{\Delta t} + \frac{1}{N_{Re}(\Delta x)^2}\left[\left(\frac{\mu^n_{i,j} + \mu^n_{i+1,j}}{2}\right) + \left(\frac{\mu^n_{i,j} + \mu^n_{i-1,j}}{2}\right)\right] \tag{14b}$$

$$C_i = \frac{\rho^n_{i,j} u^*_{i,j}}{2\,\Delta x} - \frac{1}{N_{Re}(\Delta x)^2}\left(\frac{\mu^n_{i+1,j} + \mu^n_{i,j}}{2}\right) \tag{14c}$$

For the ith column during the vertical sweep, the y-momentum equation has the form

$$A_j v^{n+1}_{i,j-1} + B_j v^{n+1}_{i,j} + C_j v^{n+1}_{i,j+1} = D_j \tag{15}$$

where

$$A_j = \frac{-\rho^*_{i,j} v^*_{i,j}}{2\,\Delta y} - \frac{1}{N_{Re}(\Delta y)^2}\left(\frac{\mu^*_{i,j} + \mu^*_{i,j-1}}{2}\right) + \frac{2}{3N_{Re}(\Delta y)^2}\left(\frac{\mu^*_{i,j} + \mu^*_{i,j-1}}{2}\right) \tag{16a}$$

$$B_j = \frac{2\rho^*_{i,j}}{\Delta t} + \frac{1}{N_{Re}(\Delta y)^2}\left[\left(\frac{\mu^*_{i,j} + \mu^*_{i,j-1}}{2}\right) + \left(\frac{\mu^*_{i,j} + \mu^*_{i,j+1}}{2}\right)\right]$$

$$- \frac{2}{3N_{Re}(\Delta y)^2}\left[\left(\frac{\mu^*_{i,j} + \mu^*_{i,j-1}}{2}\right) + \left(\frac{\mu^*_{i,j} + \mu^*_{i,j+1}}{2}\right)\right] \tag{16b}$$

$$C_j = \frac{\rho^*_{i,j} v^*_{i,j}}{2\,\Delta y} - \frac{1}{N_{Re}(\Delta y)^2}\left(\frac{\mu^*_{i,j} + \mu^*_{i,j+1}}{2}\right) + \frac{2}{3N_{Re}(\Delta y)^2}\left(\frac{\mu^*_{i,j} + \mu^*_{i,j+1}}{2}\right) \tag{16c}$$

Continuity equation.- Since the continuity equation (eq. (1)) contains no viscous terms, it was found to be beneficial in some cases to add artificial viscosity terms to equation (1) for numerical stability. These artificial viscosity terms were incorporated explicitly so that the continuity equation becomes

$$\rho_t + \rho u_x + u\rho_x + \rho v_y + v\rho_y = \alpha\left[(\Delta x)^2\rho_{xx} + (\Delta y)^2\rho_{yy}\right] \tag{17}$$

However, as described later, $\alpha = 0$ was used in many calculations. The finite-difference form of equation (17) for the horizontal sweep is then given by

$$A_i\rho^*_{i-1,j} + B_i\rho^*_{i,j} + C_i\rho^*_{i+1,j} = D_i \tag{18}$$

where

$$A_i = \frac{-u^*_{i,j}}{2\,\Delta x} + \alpha \tag{19a}$$

$$B_i = \frac{2}{\Delta t} - 2\alpha \tag{19b}$$

$$C_i = \frac{u^*_{i,j}}{2\,\Delta x} + \alpha \tag{19c}$$

For the vertical sweep, the continuity equation is given by

$$A_j\rho^{n+1}_{i,j-1} + B_j\rho^{n+1}_{i,j} + C_j\rho^{n+1}_{i,j+1} = D_j \tag{20}$$

where

$$A_j = \frac{-v_{i,j}^{n+1}}{2\,\Delta y} + \alpha \tag{21a}$$

$$B_j = \frac{2}{\Delta t} - 2\alpha \tag{21b}$$

$$C_j = \frac{v_{i,j}^{n+1}}{2\,\Delta y} + \alpha \tag{21c}$$

TEST PROBLEMS

Figure 1 shows the mixing problems (cases 1 and 2) chosen for use as the standard test problems. In these test problems, the flow is the mixing of two parallel streams where the computational region begins far downstream of the base of the infinitely thin splitter plates and is truncated farther downstream. Such a calculation obviously does not require the full Navier-Stokes equations, since solutions can be obtained with the conventional quasi-parallel approach, that is, using the boundary-layer equations with free shear flow boundary conditions. However, the test problems were chosen because solutions could be obtained with this alternate method for comparison with computed Navier-Stokes results. The test problems were also chosen because the parabolic solutions could be used to formulate and test boundary conditions. Calculations were made for the mixing of two supersonic (Mach 3 and 1.68) streams (case 1) as well as the mixing of a subsonic (Mach 0.11) stream and a supersonic (Mach 3) stream (case 2). Calculations for case 1 were made for values of N_{Re} of 10^3, 5.0×10^3, and 8.1×10^4. In all calculations for case 2, N_{Re} was 10^3.

BOUNDARY CONDITIONS

A sketch of the computational domain indicating the boundary conditions which were specified for case 2 is presented in figure 2. For case 1, the appropriate supersonic boundary conditions were applied along the entire inflow and downstream outflow boundaries.

The subsonic boundary conditions were chosen on the basis of the analysis given by Gottlieb and Gustafsson in reference 15. At the subsonic outflow boundary in case 2, the one-dimensional analysis indicated that one function value, either ρ or u, must be specified. Results of tests with three different outflow boundary conditions obtained by using an explicit method (hopscotch) given in reference 1 showed that specifying the steady-state density was the best choice. Such a boundary condition is obviously not convenient for most applications since these downstream steady-state values are generally not known

a priori. In the present investigation, however, these values were obtained from the parabolic code calculations.

The inflow profiles of u and v were also taken from parabolic code calculations. The temperature was obtained from equation (6). The density was then computed by using equation (4) with the constant value of static pressure, $p = 0.00389$.

Figure 2 also shows the arrangement of grid points at the upper and lower boundaries. At each of these locations the boundary is positioned between two rows of grid points. The specified values of u and v at the upper inflow are again obtained from the parabolic code calculations.

The linear extrapolation condition used at the downstream boundary is given for uniform grid spacing by

$$f_{NI,j} = 2f_{NI-1,j} - f_{NI-2,j} \tag{22}$$

where f is either ρ, u, or v and NI is the value of i at the downstream boundary. This is equivalent to saying that the second derivative of f is zero at NI - 1.

RESULTS AND DISCUSSION

Supersonic-Supersonic Parallel Mixing (Case 1)

Calculations were made for case 1 with $N_{Re} = 10^3$, 5.0×10^3, and 8.1×10^4. The four initial flow-field conditions that were used are as follows:

IC 1 Parabolic code inflow values for u and v specified at inflow station and outflow station; interior values obtained by linear interpolation along each row; initial density computed from equation (4) with assumption of constant static pressure; initial temperature computed from equation (6).

IC 2 Parabolic code inflow values for u and v specified at inflow station; outflow-station parabolic code values of u and v multiplied by 0.8; interior values obtained by linear interpolation along each row; initial density computed from equation (4) with assumption of constant static pressure; initial temperature computed from equation (6).

IC 3 Same as IC 2 except outflow-station parabolic code values of u and v multiplied by 0.6.

IC 4 Parabolic code inflow values for u and v specified at inflow station; initial density computed from equation (4) with assumption of constant static pressure; all interior columns and the outflow column set equal to first column; initial temperature computed from equation (6).

The solutions were considered to be converged to steady state when the following three conditions were satisfied at every point in the field:

$$\frac{1}{\Delta t}\left|u_{i,j}^{n+1} - u_{i,j}^{n}\right| \leqq 0.01\left|u_{i,j}^{n}\right| \tag{23}$$

$$\frac{1}{\Delta t}\left|v_{i,j}^{n+1} - v_{i,j}^{n}\right| \leqq 0.01\left|u_{i,j}^{n}\right| \tag{24}$$

$$\frac{1}{\Delta t}\left|\rho_{i,j}^{n+1} - \rho_{i,j}^{n}\right| \leqq 0.01\left|\rho_{i,j}^{n}\right| \tag{25}$$

This convergence criterion is identical to that of reference 1.

Calculations were presented in reference 1 for $N_{Re} = 10^3$. As shown in figure 6 of reference 1, the pressure profile exhibited pointwise oscillations. The inflow ($x = 0$) profile for that calculation was taken as the first computed profile in the parabolic solution. At $x = -0.075$ in the parabolic solution, the initial u profile was selected to be an error function between the desired outer stream velocities, u_1 and u_2. The initial v was assumed to be zero. Marching steps of $\Delta x = 0.075$ were taken. At the first computed station, $x = 0$, the v profile was still slightly affected by the inaccurate initial v profile. Another parabolic calculation was made with $\Delta x = 0.025$. Thus, the $x = 0$ station was the third station downstream and the v profile was much more accurate than in the previous solution. These new u and v profiles at $x = 0$ shown in figure 3 were used as inflow profiles in the calculations described in the present paper. Figure 3 also shows profiles from two stations farther downstream which were used as outflow boundaries in the Navier-Stokes calculations. This figure shows that the shear layer spreads significantly in the computational domain considered.

Table I summarizes the results of calculations from case 1 made with the new parabolic code profiles. The grid was 10 points (x-direction) by 122 points (y-direction) with uniform spacing $\Delta x = \Delta y = 0.025$; thus, the computational domain extended to $x_{max} = 0.225$ and to $y_{max} = 3.0125$. The computed steady-state u and v profiles at $x = 0.200$ are compared in figure 4(a) with the corresponding calculation made with the parabolic code. The circles indicate points from the parabolic calculation for which $\Delta y = 0.0125$; however, not all the points in the calculation are shown. The u profile is virtually identical to the parabolic solution. For this x-station, which is one station from the downstream boundary, the maximum difference in v in the mixing region is approximately 5 percent. The pressure profile for the station shown in figure 4(b) is smooth and indicates only a slight deviation (about 1 percent) in the mixing region from the constant value (indicated by the dashed line) assumed in the parabolic calculation. Thus, the use of the new, more accurate inflow profiles removed the pointwise pressure oscillations present in the calculations of reference 1.

Effect of Courant number.- The time step used in the previously described calculation was 0.7 times the maximum step allowed for stability in the explicit hopscotch method, that is, $N_{Co} = 0.7$ where

$$N_{Co} = \frac{\Delta t}{\frac{\Delta x}{|u| + |v| + \sqrt{2}c}} \tag{26}$$

Since u varies throughout the domain, the time-step size is actually governed by the maximum value of u which is u_2. For $N_{Co} = 1.0$ (Courant-Freidrichs-Lewy condition) for case 1, Δt was 0.021. For $N_{Co} = 0.7$, steady-state convergence was obtained in 329 steps. As shown in table I, as N_{Co} was increased to 5.0, the number of steps required for convergence dropped to 62. In all these calculations, initial condition IC 1 was used and Δt was held constant for all time-marching steps. For $N_{Co} = 10.0$, however, the solution diverged. A possible cause of this divergence was roundoff error from the tridiagonal matrix inversion occurring when the coefficient matrix did not possess diagonal dominance. The diagonal dominance condition, that is,

$$|B_i| \geq |A_i| + |C_i| \tag{27}$$

is a sufficient but not necessary condition for convergence of the matrix reduction. Keller (ref. 16) presents an inductive proof that diagonal dominance insures no error growth in the Thomas algorithm. Hirsh and Rudy discuss diagonal dominance further in reference 17. In the present $N_{Co} = 10.0$ calculation, the continuity equation was not diagonally dominant for any row in the horizontal sweep. In addition, the two momentum equations lacked diagonal dominance for many rows.

Even very large time steps were not possible when the initial flow field was taken to be the converged steady-state flow field. A calculation was made in which N_{Co} was increased by a factor of 1.05 every time step starting with $N_{Co} = 1.0$. When N_{Co} reached 54.6, the solution began to diverge rapidly in the next few time steps.

Effect of downstream boundary condition.- To test the effect of the linear extrapolation outflow boundary conditions, a calculation was made for case 1 with $N_{Re} = 10^3$, $\alpha = 0$, and $N_{Co} = 1.0$ with 20 x-stations instead of 10 so that the domain extended to $x = 0.475$. The u and v profiles at $x = 0.200$ (a station which was now near the middle of the domain instead of one column from the boundary) were virtually identical to those of the previous calculation. The maximum difference in u was less than 0.5 percent and for v less than 1.0 percent. Thus, for this problem, linear extrapolation is a reasonable boundary condition.

Comparison with explicit method.- The ADI results for case 1 with $N_{Re} = 10^3$ were compared with solutions of the same equations in the same computational domain

obtained by using the explicit hopscotch method described in reference 1. For $N_{Co} = 0.7$, the hopscotch solution required 238 steps to reach steady-state convergence. The computed steady-state flow fields were virtually identical, with maximum differences of much less than 1 percent. For each time step, the CPU time on the Control Data 6600 computer system for hopscotch was 1.08×10^{-3} sec/node, and for the ADI method, 3.74×10^{-3} sec/node. (Neither code was optimized.) The best ADI solution (62 steps for $N_{Co} = 5.0$) took about one-fourth as many steps as the hopscotch method, so that the total CPU time for the two methods was comparable. (The hopscotch method was unstable for $N_{Co} = 0.9$ for this problem.)

Effect of initial conditions.- Calculations were also made with initial conditions which were not considered to be as good an approximation to the steady-state result as was IC 1. The steady-state downstream values of u and v were multiplied by 0.8 in IC 2 and 0.6 in IC 3. Linear interpolation was again used to compute interior values. As shown in table I, convergence was actually reached 10 steps sooner with IC 2 and 30 steps later with IC 3 than with IC 1. However, in both cases the steady-state flow fields were identical to the one computed for IC 1.

Effect of increased Reynolds number.- The results of calculations for case 1 with $N_{Re} = 5.0 \times 10^3$ from reference 1 are shown in figure 5. (It should be noted that in fig. 7 of ref. 1 these plots were incorrectly captioned as being for subsonic-supersonic mixing.) As shown in figure 5(a), with $\Delta x = \Delta y = 0.025$ (10×122 grid), the u profile at $x = 0.15$ was accurately predicted, whereas the v profile exhibited an oscillation near its maximum value in the viscous mixing region. Halving the grid so that $\Delta x = \Delta y = 0.0125$ (19×122 grid) eliminated this oscillation. The pressure profiles shown in figure 5(b) have small pointwise oscillations for both grids although the maximum deviation from the parabolic code value is less for the finer grid. New initial profiles were also generated for case 1 ($N_{Re} = 5.0 \times 10^3$) by recomputing the parabolic solution with a smaller Δx step. As before, the parabolic solution initial profile for u was an error-function curve fit between u_1 and u_2; a zero-v initial profile was used. The results from the ADI calculations with these new inputs are summarized in table II. A 19×122 grid was again used with x extending to 0.225 and y extending to 1.50625. A comparison of velocity profiles with the parabolic calculation for the mixing region is shown in figure 6(a) for $x = 0.15$. Excellent agreement is again obtained for both u and v. As shown in figure 6(b), the new pressure profile is smoother than the reference 1 profile although very slight oscillations are still present. (The y values of the ref. 1 profile have been shifted in fig. 6(b) to correspond to those of the new calculation.) The deviation from the free-stream value is still much less than 1 percent.

For $N_{Co} = 0.9$, the ADI solution required approximately five times as many steps to reach steady state as the solution with the hopscotch method. For $N_{Co} = 0.9$, the new

inflow profiles did not affect the convergence rate; however, for $N_{Co} = 5.0$, ADI required 103 steps (3 times as many as hopscotch) with the new inputs instead of the previous 134 steps. The solution diverged for $N_{Co} = 10.0$. This divergence was again possibly due to the loss of diagonal dominance in one or more of the coefficient matrices.

Some tests were also made for case 1 with $N_{Re} = 5.0 \times 10^3$ to determine the effect of adding artificial viscosity to the continuity equation. In reference 1, it was shown that small values of α in equation (17) smoothed the pressure in the hopscotch calculations of case 2 at a higher Reynolds number. With $\alpha = 0.25$ and 0.50, the u and v profiles were not altered for $N_{Co} = 0.9$ while the slight pressure oscillations were smoothed. For $\alpha = 0.50$, the oscillation was reduced to one point. However, as indicated in table II, the convergence rate decreased about 10 percent as α was increased from 0 to 0.5. In addition, for $N_{Co} = 5.0$, a computation with $\alpha = 0.5$ also diverged as had the computation with $\alpha = 0$. For all computations in which artificial viscosity was used, a constant value of α was used during the entire calculation.

Calculations were also made for case 1 with $N_{Re} = 8.1 \times 10^4$. A 19×122 grid ($x_{max} = 0.225$ and $y_{max} = 1.50625$) was again used and inflow profiles were generated by using the parabolic code. The results are listed in table II and the computed steady-state profiles are shown in figure 7 for $x = 0.1875$, a station near the outflow boundary. The agreement with the parabolic solution is very good; for example, the maximum deviation from the free-stream pressure is less than 0.1 percent. Even though the shear layer spreads only slightly over the solution domain considered, this calculation demonstrates that the ADI method is stable for significantly high Reynolds number flows. Initial condition IC 1 for this flow gives a flow field which closely approximates the steady-state flow field; however, over 600 steps were needed to reach steady state with $\alpha = 0.25$. A solution with $\alpha = 0$ was run but convergence at all grid points was not obtained after 1800 time steps. The calculation was not continued further. The solution diverged for $N_{Co} = 5.0$.

Effect of diagonal dominance.- Two other forms of spatial differencing which give diagonally dominant coefficient matrices were also investigated. These forms were upwind differencing and the differencing scheme of Khosla and Rubin.

Upwind differencing: In upwind differencing, one-sided, rather than centered, finite-difference approximations were used for the convective terms in the continuity equation and the two momentum equations. For example, the term $\rho v u_y$ was differenced as

$$(\rho v)_{i,j}\left(\frac{u_{i,j} - u_{i,j-1}}{\Delta y}\right) \qquad \left(v_{i,j} > 0\right)$$

and

$$(\rho v)_{i,j}\left(\frac{u_{i,j+1} - u_{i,j}}{\Delta y}\right) \qquad \left(v_{i,j} < 0\right)$$

Thus, the one-sided difference is always taken on the upstream, or upwind, side of the point at which the derivative is being computed. This technique has been used extensively in previous numerical calculations. Roache (ref. 8) discusses many of these applications in detail. The elimination of central differencing for first derivatives gives diagonally dominant coefficient matrices in all three difference equations for both sweeps.

Upwind differencing was used to compute case 1 with $N_{Re} = 10^3$. These results are listed in table I. For $N_{Co} = 1.0$, convergence was obtained in 132 steps, which is about one-third as many steps as with central differencing. For $N_{Co} = 5.0$, only 30 steps were needed; this is less than one-half the number required for central differencing $(N_{Co} = 5.0)$ and one-eighth the number for hopscotch $(N_{Co} = 0.7)$. In both computations with upwind differencing, the u profiles were virtually identical to those in the central differencing calculation, and the v profiles differed by less than 2 percent in the mixing region. As with central differencing, the pressure deviates from the free-stream value by less than 1 percent. Apparently Δx and Δy were sufficiently small that the first-order differencing did not significantly alter the results. Although the numerical diffusion introduced by upwind differencing did not affect the profiles, it may have been at least partially responsible for the improved convergence rate.

A converged solution could not be obtained for $N_{Co} = 10.0$, as was the case with central differencing. Oscillations which appeared early in the solution in all variables eventually resulted in divergence. The exact cause of these oscillations is not known, but it obviously is not the loss of diagonal dominance.

The results for case 1 with $N_{Re} = 5.0 \times 10^3$ are listed in table II. For $N_{Co} = 5.0$, only 48 steps were needed to reach steady state. As with $N_{Re} = 10^3$, the use of upwind differencing reduced the total number of steps required by a factor of 2. The u, v, and ρ profiles are again virtually identical to the central differencing results. The artificial viscosity inherent in the upwind differencing did not smooth the small pointwise pressure oscillations shown in figure 6(b). As with central differencing, the solution diverged for $N_{Co} = 10.0$.

For the highest Reynolds number, $N_{Re} = 8.1 \times 10^4$, the upwind solution converged almost four times as fast as the central differencing solution for $N_{Co} = 1.0$. As shown in table II, adding artificial viscosity improved the convergence rate slightly.

Khosla-Rubin differencing: Another indication that divergence is not always caused by a loss of diagonal dominance was given by the results of tests using the differencing scheme of Khosla and Rubin (ref. 18). This method, which is second-order accurate and unconditionally diagonally dominant, uses a modified differencing for convective terms instead of central differencing. For example, for the term $\rho v u_y$, the differencing becomes

$$(\rho v)^n_{i,j}\left[\left(\frac{u^{n+1}_{i,j} - u^{n+1}_{i,j-1}}{\Delta y}\right) + \left(\frac{u^n_{i,j+1} - 2u^n_{i,j} + u^n_{i,j-1}}{2\,\Delta y}\right)\right] \qquad \left(v_{i,j} > 0\right)$$

and

$$(\rho v)^n_{i,j}\left[\left(\frac{u^{n+1}_{i,j+1} - u^{n+1}_{i,j}}{\Delta y}\right) - \left(\frac{u^n_{i,j+1} - 2u^n_{i,j} + u^n_{i,j-1}}{2\,\Delta y}\right)\right] \qquad \left(v_{i,j} < 0\right)$$

This expression reduces to the usual central differencing at steady state when $u^{n+1}_{i,j} = u^n_{i,j}$. In the present application it was used only for the implicit convective terms in each equation; the central differencing form was retained in the D_j and D_i terms. The method was shown to be unconditionally stable for a one-dimensional model equation (Burgers' equation) in reference 18 using a linear stability analysis.

As shown in table I, for case 1 with $N_{Re} = 10^3$, steady state was reached in 129 steps for $N_{Co} = 1$; this is approximately the same number of steps required with upwind differencing. The u and v profiles were again essentially identical to the central differencing results, and the pressure again deviated from the free-stream value by less than 1 percent. For $N_{Co} = 5.0$, however, oscillations developed in the solution which produced a rapid divergence even though diagonal dominance was maintained. The same result occurred with $N_{Re} = 5.0 \times 10^3$ and $N_{Co} = 5.0$. Similar behavior was observed in solutions of the nonconservative form of the nonlinear Burgers' equation (ref. 19) but not for the linear Burgers' equation even when "wiggles" were present in the solution. Thus, these examples suggest that the method may not always be stable for nonlinear equations.

Subsonic-Supersonic Parallel Mixing (Case 2)

Calculations for case 2 were made with central and upwind differencing with $N_{Re} = 10^3$. The boundary conditions shown in figure 2 were used with necessary specified values obtained from the parabolic solution. The grid was 10×122 with $\Delta x = \Delta y = 0.05$ so that $x_{max} = 0.450$ and $y_{max} = 6.025$. Initial condition IC 1 was used for all calculations. The results of the calculations are summarized in table III.

The computed steady-state velocity profiles at $x = 0.15$ are compared in figure 8(a) with the corresponding calculation obtained by using the parabolic code. The u profile is virtually identical to the parabolic solution, and the v profile shows very good agreement. This agreement is also very good at all other x-stations in the solution domain. The static-pressure profiles at two stations, $x = 0.15$ and 0.30, are shown in figure 8(b). The maximum deviation from free-stream static pressure occurs near the sonic point close to

the inflow boundary. As shown, the maximum deviation decreases with downstream distance. These pressure profiles were smooth with no pointwise oscillations. Gottlieb and Gustafsson (ref. 15) observed pressure oscillation in their hopscotch calculation of a shear layer flow with a larger transonic region. They were able to smooth the pressure by altering the subsonic inflow boundary conditions through specification of appropriate characteristic variables at the boundaries. Although the pressure does not oscillate spatially in the present calculation, incorporation of the Gottlieb-Gustafsson boundary condition may improve the pressure near the sonic point in the ADI calculations.

With central differencing it was necessary to use some artificial viscosity in the continuity equation to obtain convergence. With $\alpha = 0$, the solution for $N_{Co} = 0.5$ diverged after 600 time steps; however, with $\alpha = 0.75$, the solution converged in 807 steps. Hopscotch required 683 steps to obtain convergence for $N_{Co} = 0.5$ and $\alpha = 0.25$. (Artificial viscosity was also needed with hopscotch.) As shown in table III, the number of time steps required decreased as N_{Co} was increased. For $N_{Co} = 5.0$, only 100 time steps were required for convergence. The solution diverged when $N_{Co} = 10.0$. It can also be noted from these results that the presence of subsonic flow increased the total number of time steps required in comparison with the fully supersonic case 1 results with $N_{Re} = 10^3$.

ADI with upwind differencing required no artificial viscosity (i.e., $\alpha = 0$) for $N_{Co} = 2.5$. Steady state was reached in 95 steps, which is about one-seventh of the steps required for hopscotch for $N_{Co} = 0.5$. No solution could be obtained for $N_{Co} = 4.0$ with $\alpha = 0$, 0.25, or 0.75.

CONCLUDING REMARKS

A sequential (uncoupled) time-asymptotic finite-difference alternating-direction implicit (ADI) method was tested on laminar parallel free mixing flows by using the compressible Navier-Stokes equations. For the mixing of two supersonic streams with a Reynolds number of 10^3, a converged steady-state flow field was computed with a Courant number of 5.0 and central differencing. The solution diverged for a Courant number of 10.0, caused perhaps by the loss of diagonal dominance in the coefficient matrices of the governing equations. There are other factors, however, which may also have affected the size of the maximum allowable time step. For example, the effect of lagging the pressure and cross-derivative terms is not known. In addition, the nonlinear coefficients in the convective terms were lagged in order to linearize the equations. Such a linearization may only be appropriate for small time steps. Therefore, a fully coupled procedure with a better linearization technique may be needed to gain somewhat larger time steps.

Two procedures which give unconditional diagonal dominance were also tested and both were found to be limited in allowable time step size. Solutions with upwind differencing of the convective terms diverged for a Courant number of 10.0; whereas solutions with the Khosla-Rubin method diverged for a Courant number of 5.0. In both of these solutions the failure cannot be attributed to the loss of diagonal dominance. It appears that the methods are not unconditionally stable for the full nonlinear Navier-Stokes equations, as the linear stability analysis for model equations indicates, but further research is required before a definite conclusion can be reached. Perhaps some alternate form of linearization may give a more stable scheme even with an uncoupled solution procedure.

The use of upwind differencing in the ADI method significantly improved the convergence rate. With a Courant number of 5.0, the upwind version of ADI converged in about one-half the number of time steps required with central differencing and one-eighth the number required by the explicit hopscotch method. Thus, the expected advantage of an implicit method was realized for the supersonic mixing case with a Reynolds number of 10^3. When the Reynolds number was raised to 5.0×10^3, the hopscotch method proved to be superior to the ADI in terms of convergence rate and total computing time.

The ADI method also converged in less total computing time than hopscotch for the parallel mixing of a subsonic stream with a supersonic stream for a Reynolds number of 10^3. Thus, it appears that ADI can be competitive with explicit methods for some problems with regard to total computing time; however, the ADI method requires more than twice the computer storage that hopscotch requires, and ADI is more complex to code than most explicit methods. This result cannot, of course, be generalized until comparisons are made over a wider range of flow problems.

With central differencing for the convective terms, it was necessary to add artificial viscosity to the continuity equation to obtain convergence for subsonic-supersonic mixing. None was needed, however, for upwind differencing, which inherently possesses some artificial viscosity. For completely supersonic mixing, artificial viscosity was necessary only for the highest Reynolds number, 8.1×10^4, when central differencing was used.

The very large time steps which were expected prior to the present investigation were not possible for the uncoupled procedure for the test problems considered. A fully coupled solution technique may not yield a significantly larger time step than an uncoupled procedure. For nonlinear equations, the high-frequency waves in the solution domain are coupled with the low-frequency waves. These high-frequency waves can grow undamped and lead to divergence if the solution and/or method parameters are not highly smooth. It is possible that too large a time step may adversely alter the wavelength of information

coming into the solution domain and cause such a divergence. If this happens, coupling the equations will probably not prevent the divergence and allow larger time steps.

Langley Research Center
National Aeronautics and Space Administration
Hampton, VA 23665
August 3, 1976

REFERENCES

1. Rudy, David H.; Morris, Dana J.; Blanchard, Doris K.; Cooke, Charlie H.; and Rubin, Stanley G.: An Investigation of Several Numerical Procedures for Time-Asymptotic Compressible Navier-Stokes Solutions. Aerodynamic Analyses Requiring Advanced Computers, Part I, NASA SP-347, 1975, pp. 437-468.

2. Peyret, Roger; and Viviand, Henri: Computation of Viscous Compressible Flows Based on the Navier-Stokes Equations. AGARD-AG-212, Sept. 1975.

3. Taylor, T. D.: Numerical Methods for Predicting Subsonic, Transonic and Supersonic Flow. AGARDograph No. 187, Jan. 1974.

4. Peaceman, D. W.; and Rachford, H. H., Jr.: The Numerical Solution of Parabolic and Elliptic Differential Equations. J. Soc. Ind. & Appl. Math., vol. 3, no. 1, Mar. 1955, pp. 28-41.

5. Douglas, Jim, Jr.: On the Numerical Integration of $\frac{\partial^2 u}{\partial x^2} + \frac{\partial^2 u}{\partial y^2} = \frac{\partial u}{\partial t}$ by Implicit Methods. J. Soc. Ind. & Appl. Math., vol. 3, no. 1, Mar. 1955, pp. 42-65.

6. Von Rosenberg, Dale U.: Methods for the Numerical Solution of Partial Differential Equations. American Elsevier Pub. Co., Inc., 1969.

7. Gourlay, A. R.; and Mitchell, A. R.: Alternating Direction Methods for Hyperbolic Systems. Numer. Math., Bd. 8, Heft 2, Apr. 4, 1966, pp. 137-149.

8. Roache, Patrick J.: Computational Fluid Dynamics. Hermosa Publ., c.1972.

9. Polezhaev, V. I.: Numerical Solution of the System of Two-Dimensional Unsteady Navier-Stokes Equations for a Compressible Gas in a Closed Region. Fluid Dyn., vol. 2, Mar.-Apr. 1967, pp. 70-74.

10. Briley, W. R.; and McDonald, H.: An Implicit Numerical Method for the Multidimensional Compressible Navier-Stokes Equations. Rep. M911363-6 (Contract No. N00014-72-C-0183), United Aircraft Res. Lab., United Aircraft Corp., Nov. 1973. (Available from DDC as AD 770 224.)

11. Douglas, Jim, Jr.; and Gunn, James E.: A General Formulation of Alternating Direction Methods. Part I. Parabolic and Hyperbolic Problems. Numer. Math., Bd. 6, 1964, pp. 428-453.

12. Baum, Eric; and Ndefo, Ejike: A Temporal ADI Computational Technique. AIAA Computational Fluid Dynamics Conference, July 1973, pp. 133-140.

13. Baum, E.: Final Technical Report – Turbulent Wakes. 23028-6002-RU-00 (Contract No. N00014-72-C-0448), TRW Syst. Group, TRW Inc., Dec. 31, 1973.

14. Oh, Y. H.: Analysis of Two-Dimensional Free Turbulent Mixing. AIAA Paper No. 74-594, June 1974.

15. Gottlieb, David; and Gustafsson, Bertil: On the Navier-Stokes Equations With Constant Total Temperature. NASA CR-132664, 1975.

16. Keller, Herbert B.: Numerical Methods for Two-Point Boundary-Value Problems. Blaisdell Pub. Co., c.1968.

17. Hirsh, Richard S.; and Rudy, David H.: The Role of Diagonal Dominance and Cell Reynolds Number in Implicit Difference Methods for Fluid Mechanics Problems. J. Comput. Phys., vol. 16, no. 3, Nov. 1974, pp. 304-310.

18. Khosla, P. K.; and Rubin, S. G.: A Diagonally Dominant Second-Order Accurate Implicit Scheme. Comput. & Fluids, vol. 2, no. 2, Aug. 1974, pp. 207-209.

19. Rudy, David H.; and Hirsh, Richard S.: Comments on the Role of Diagonal Dominance in Implicit Difference Methods. NASA TM X-73905, 1976.

TABLE I.- SUMMARY OF RESULTS FROM CALCULATIONS FOR CASE 1 AT $N_{Re} = 10^3$

[$\Delta x = \Delta y = 0.025$; $x_{max} = 0.225$; grid dimensions, 10×122]

N_{Co}	IC	α	Time steps required for convergence			
			ADI central	ADI upwind	ADI Khosla-Rubin	Hopscotch
0.7	1	0	329			238
1.0	1	0	202	132	129	
5.0	1	0	62	30	Diverged	
10.0	1	0	Diverged	Diverged		
.7	2	0	319			
.7	3	0	352			

TABLE II.- SUMMARY OF RESULTS FROM CALCULATIONS FOR CASE 1 AT HIGH REYNOLDS NUMBERS

[$\Delta x = \Delta y = 0.0125$; $x_{max} = 0.225$; grid dimensions, 19×122]

N_{Re}	N_{Co}	IC	α	Time steps required for convergence			
				ADI central	ADI upwind	ADI Khosla-Rubin	Hopscotch
5.0×10^3	0.9	4	0	168			33
	.9	4	.25	175			
	.9	4	.5	184			
	5.0	4	0	103	48	Diverged	
	10.0	4	0	Diverged	Diverged		
	10.0	4	.5	Diverged			
8.1×10^4	1.0	1	.25	666	183		
	5.0	1	.25	Diverged	Diverged		
	1.0	1	0		199		

TABLE III.- SUMMARY OF RESULTS FROM CALCULATIONS FOR CASE 2 AT $N_{Re} = 10^3$

[$\Delta x = \Delta y = 0.05$; $x_{max} = 0.450$; grid dimensions, 10×122]

N_{Co}	IC	α	Time steps required for convergence		
			ADI central	ADI upwind	Hopscotch
0.5	1	0	Diverged		
.5	1	.25			683
.5	1	.75	807		
.9	1	.75	621		
2.5	1	0		95	
4.0	1	.75		Diverged	
5.0	1	.75	100		
10.0	1	.75	Diverged		

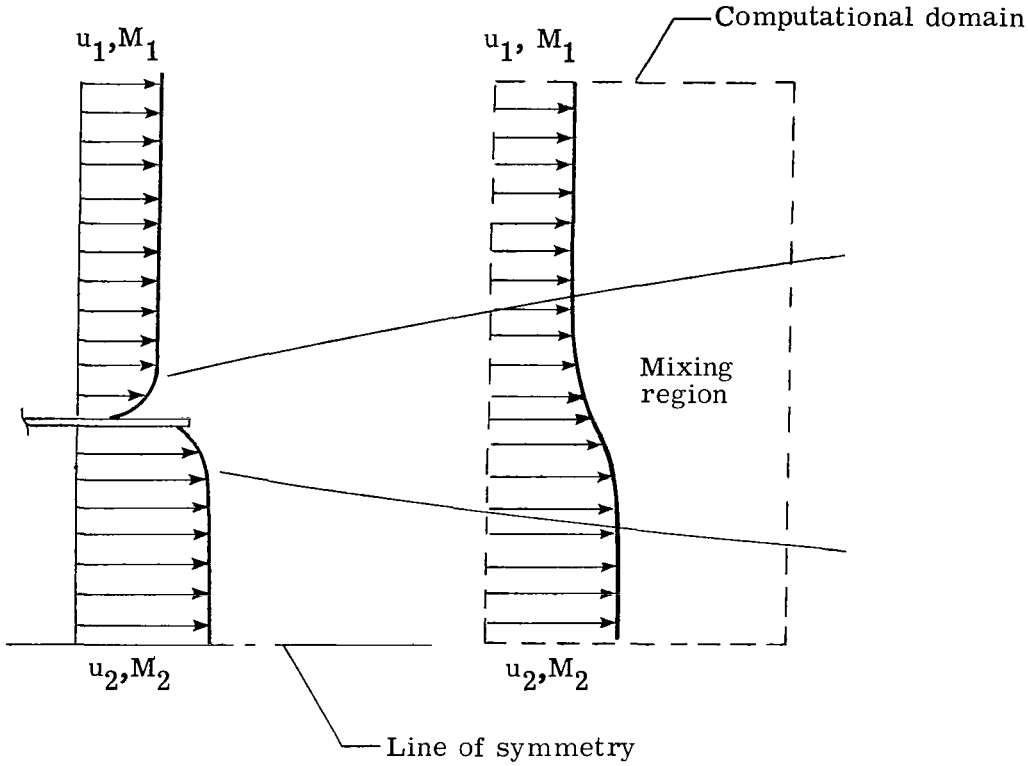

Case 1	Case 2
$M_1 = 1.68$	$M_1 = 0.11$
$M_2 = 3.00$	$M_2 = 3.00$

Figure 1.- Standard test problems for mixing of two parallel streams.

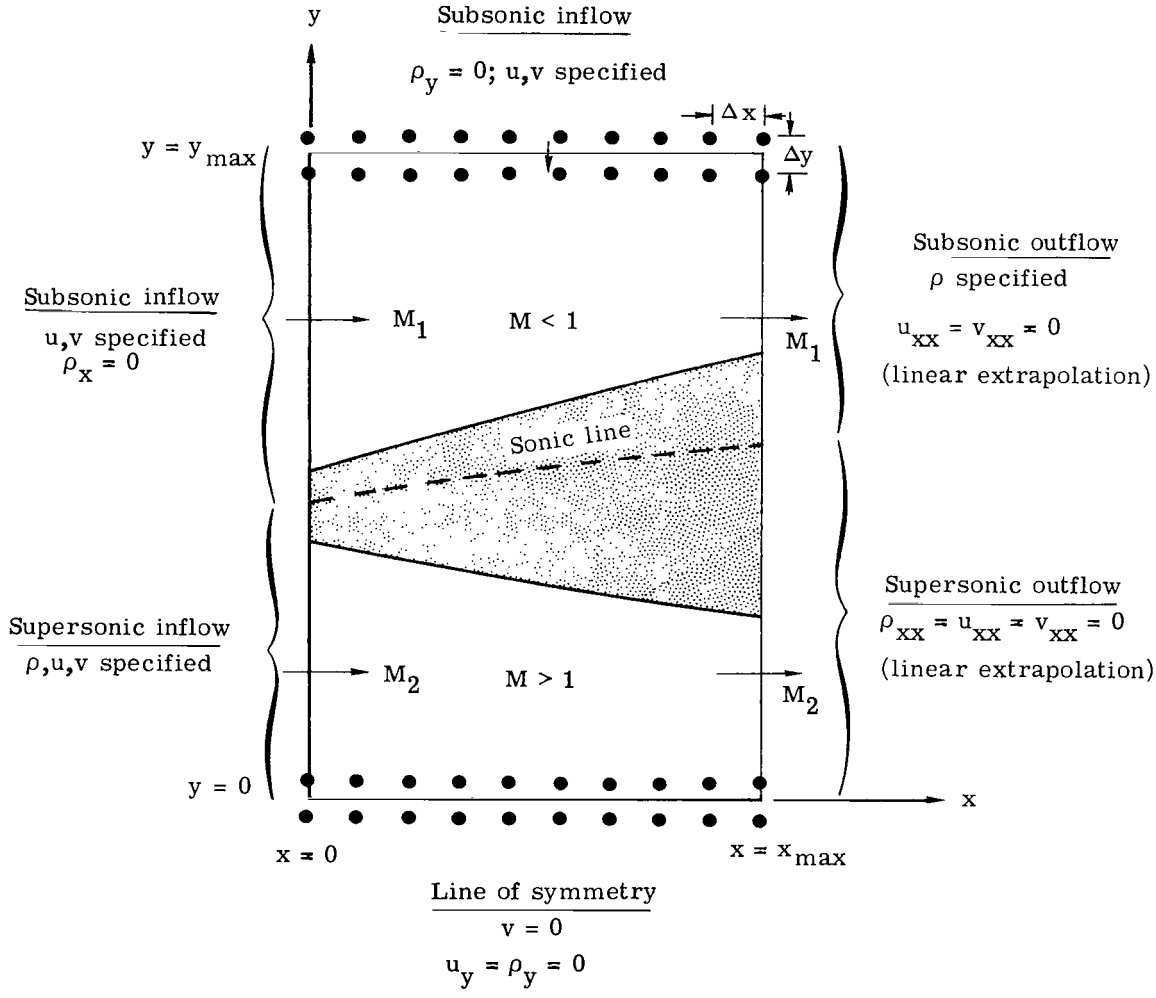

Figure 2.- Schematic of computational domain with boundary conditions for case 2 and grid alinement at upper and lower boundaries.

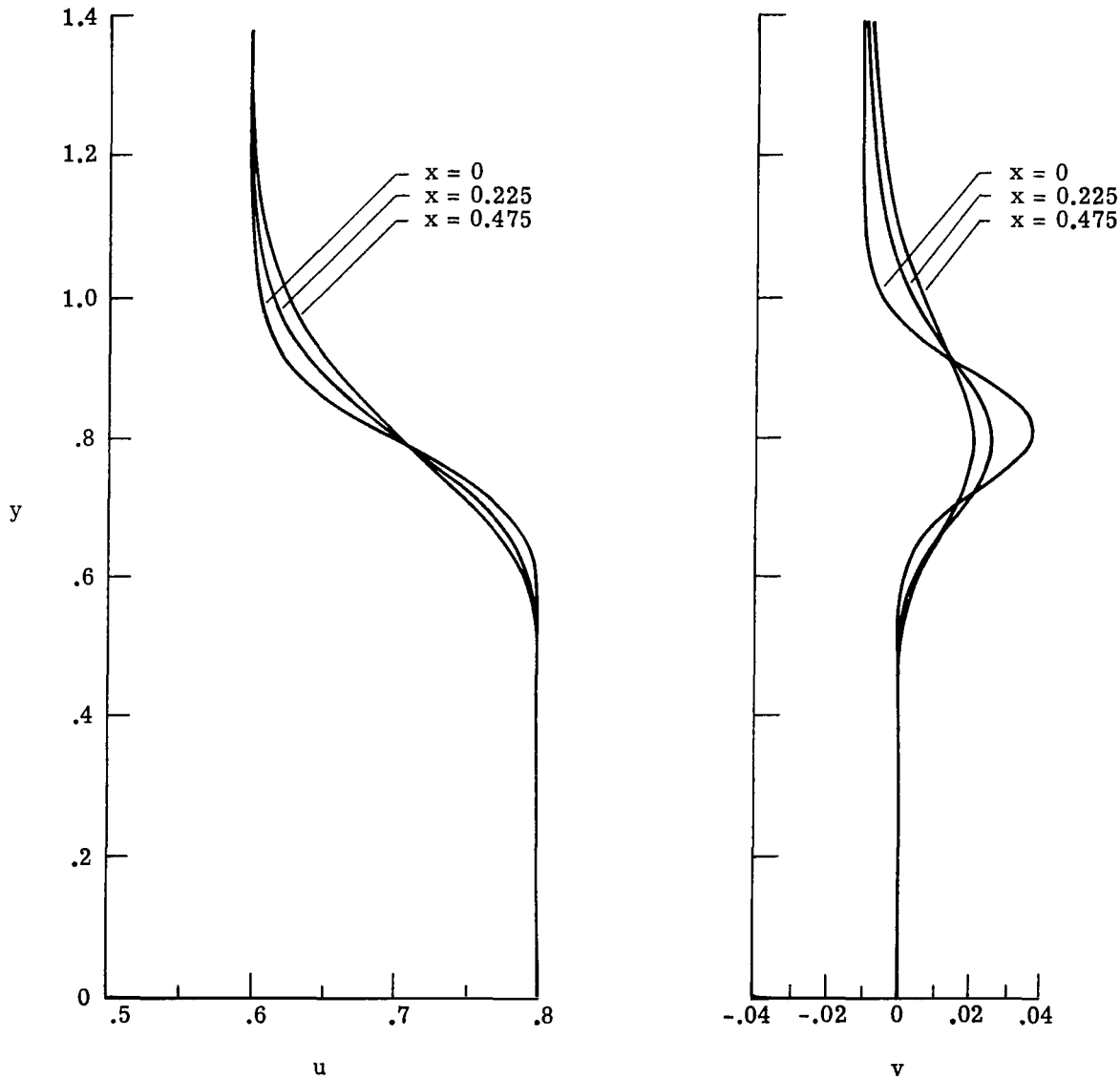

Figure 3.- Velocity profiles for case 1 for $N_{Re} = 10^3$ computed with parabolic shear layer code of reference 14.

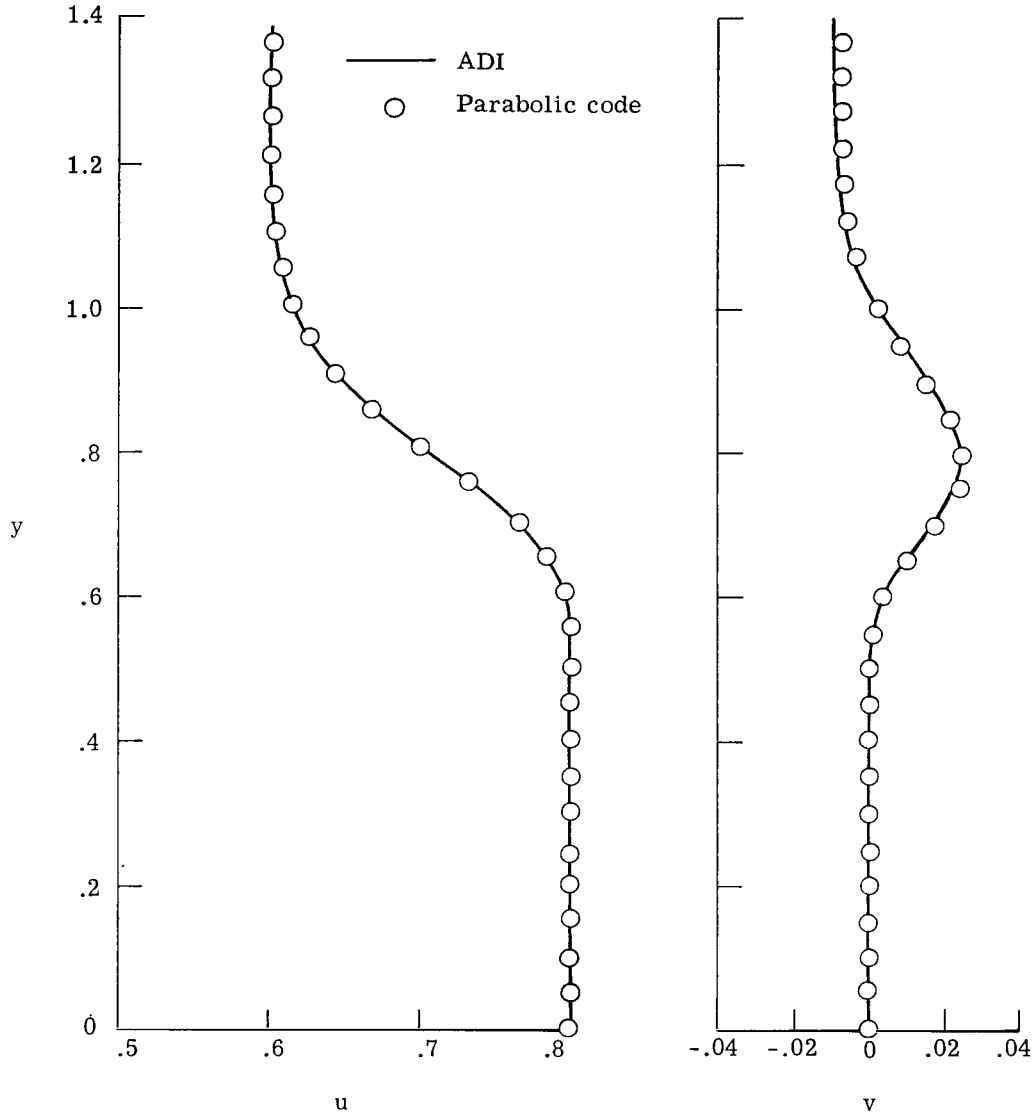

(a) Steady-state velocity profiles.

Figure 4.- Supersonic-supersonic (case 1) mixing for $N_{Re} = 10^3$. $\Delta x = \Delta y = 0.025$; $x = 0.200$.

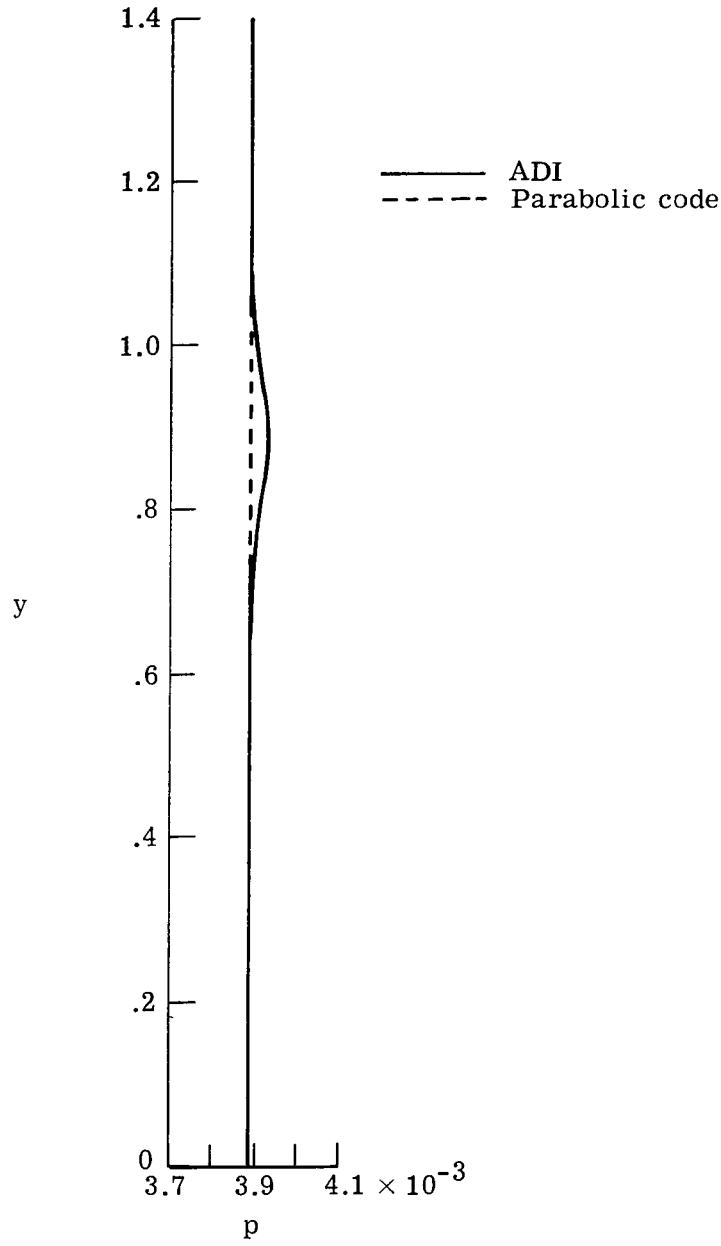

(b) Steady-state pressure profile.

Figure 4.- Concluded.

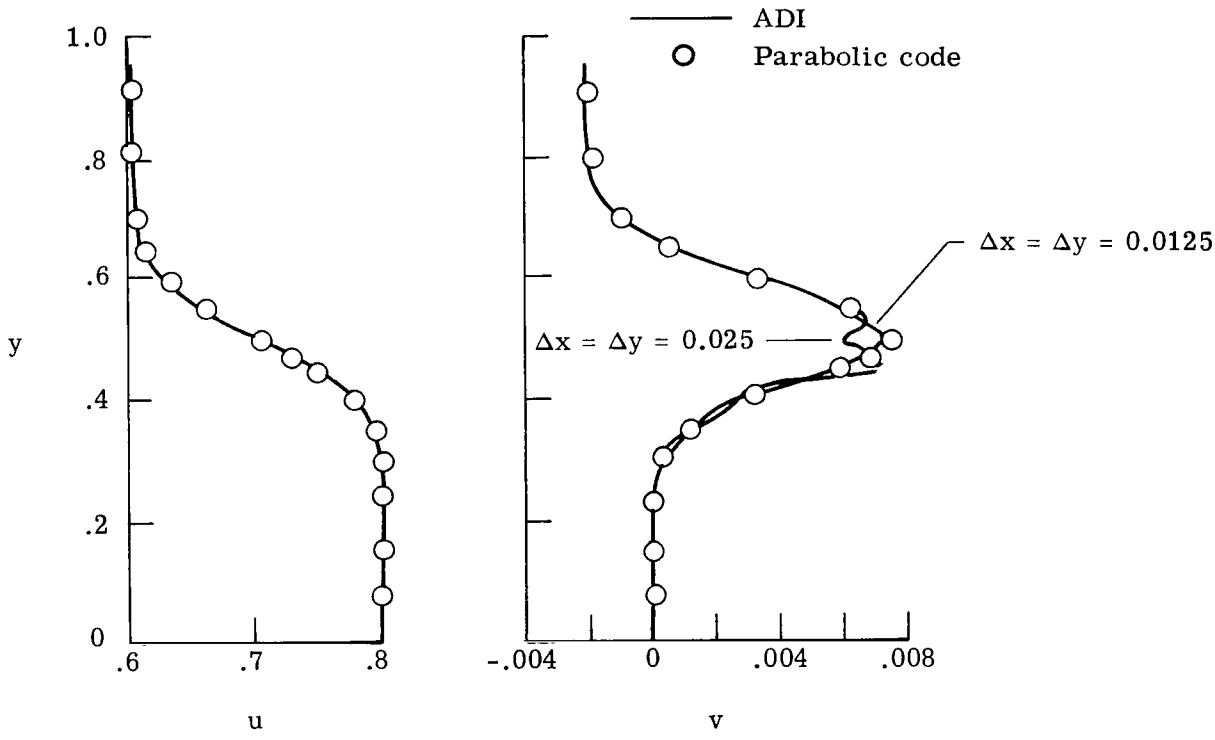

(a) Steady-state velocity profiles.

Figure 5.- Supersonic-supersonic (case 1) mixing for $N_{Re} = 5.0 \times 10^3$. x = 0.15. (Calculation from ref. 1.)

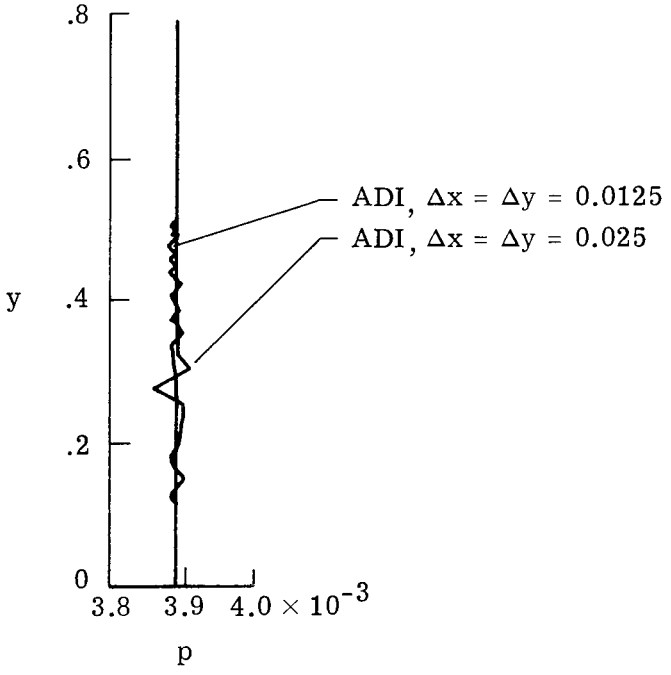

(b) Steady-state pressure profiles.

Figure 5.- Concluded.

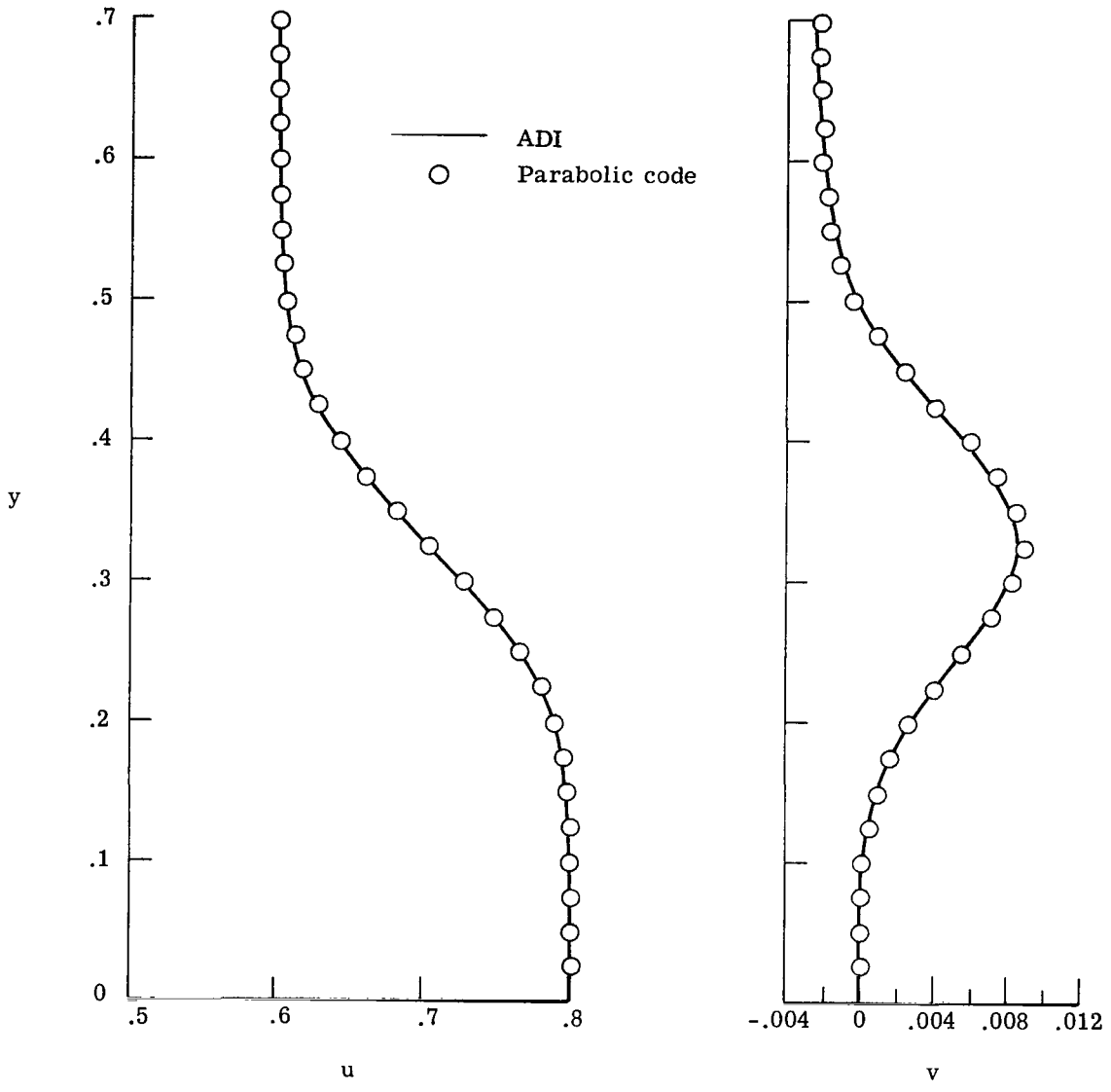

(a) Steady-state velocity profiles.

Figure 6.- Supersonic-supersonic (case 1) mixing for $N_{Re} = 5.0 \times 10^3$. x = 0.15; improved inflow profiles.

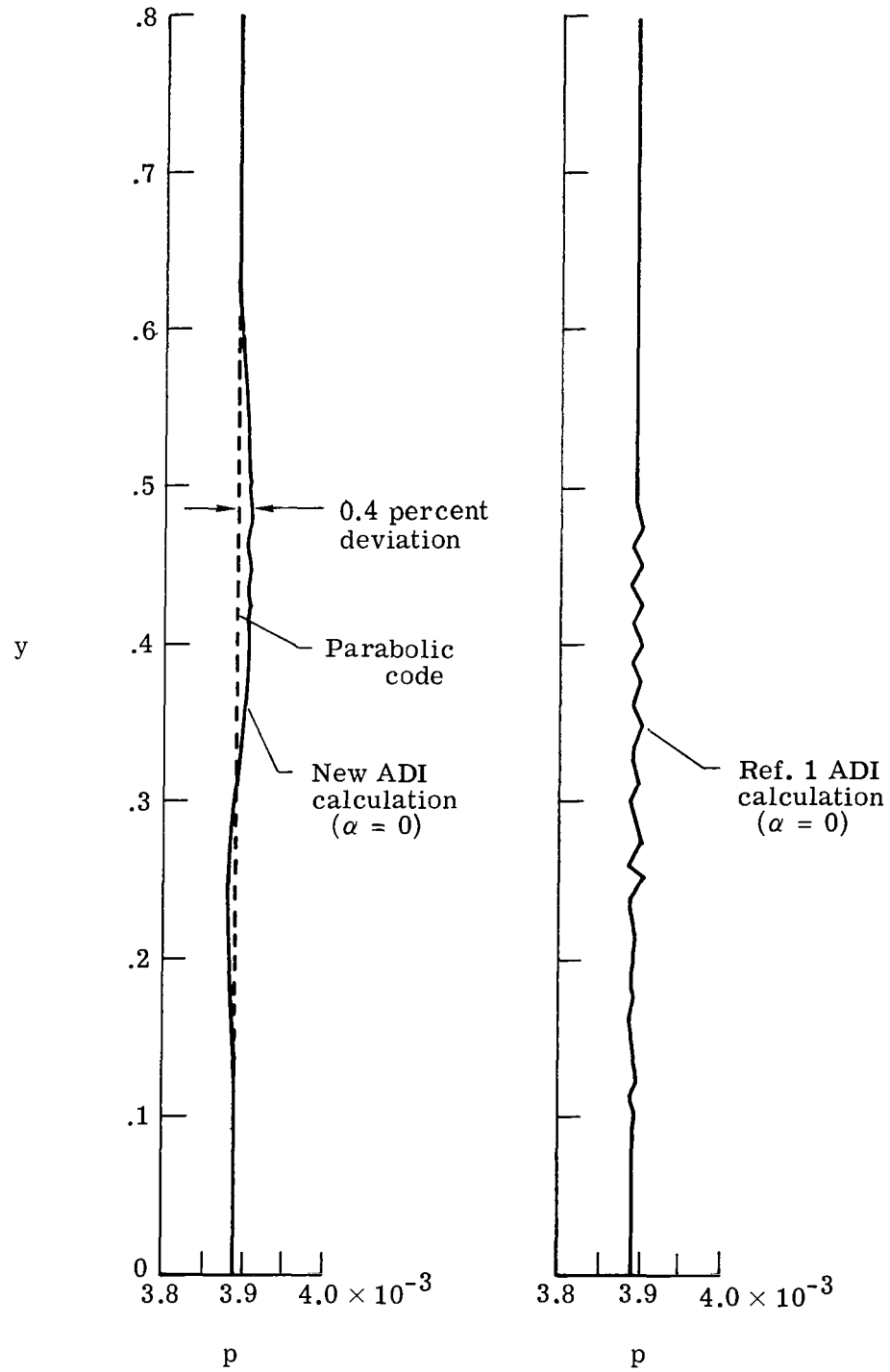

(b) Steady-state pressure profiles.

Figure 6.- Concluded.

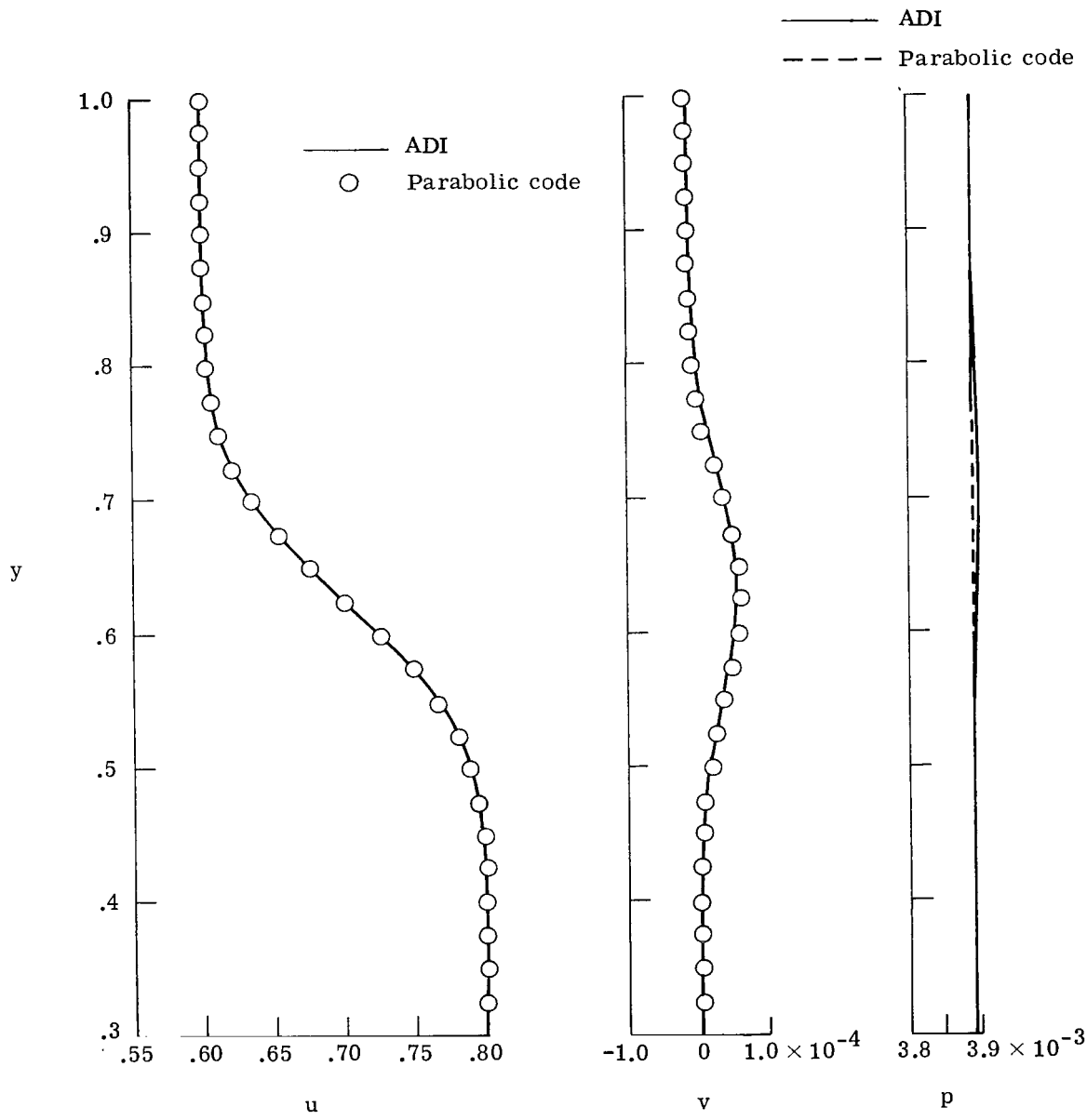

Figure 7.- Supersonic-supersonic (case 1) mixing for $N_{Re} = 8.1 \times 10^4$. x = 0.1875; steady-state profiles; $\alpha = 0.25$.

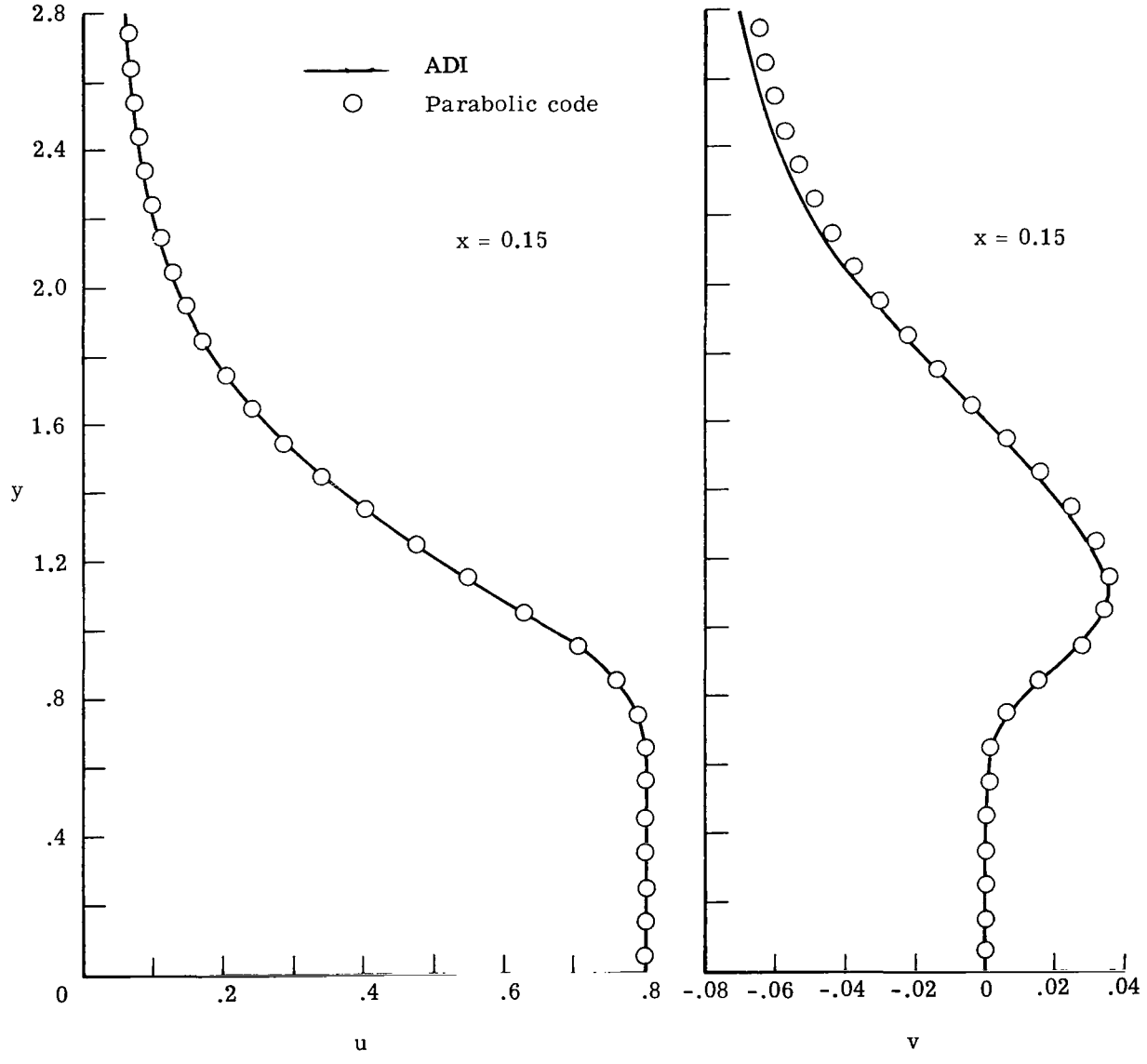

(a) Steady-state velocity profiles.

Figure 8.- Subsonic-supersonic (case 2) mixing for $N_{Re} = 10^3$.
$\Delta x = \Delta y = 0.05$; $\alpha = 0.75$.

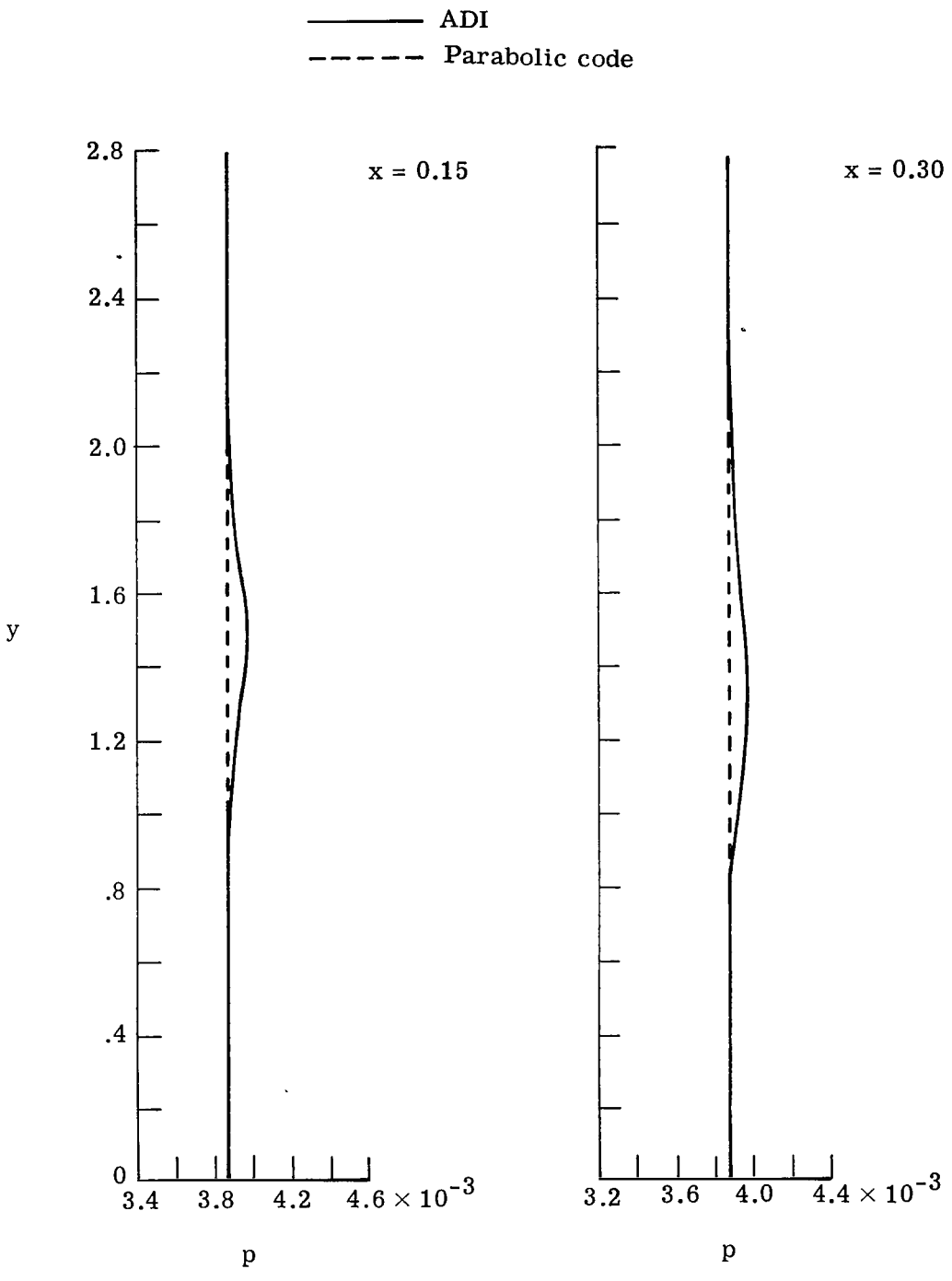

(b) Steady-state pressure profiles.

Figure 8.- Concluded.

NATIONAL AERONAUTICS AND SPACE ADMINISTRATION
WASHINGTON, D.C. 20546

OFFICIAL BUSINESS
PENALTY FOR PRIVATE USE $300

SPECIAL FOURTH-CLASS RATE BOOK

POSTAGE AND FEES PAID
NATIONAL AERONAUTICS AND SPACE ADMINISTRATION
451

U.S.MAIL

807 001 C1 U D 760924 S00903DS
DEPT OF THE AIR FORCE
AF WEAPONS LABORATORY
ATTN: TECHNICAL LIBRARY (SUL)
KIRTLAND AFB NM 87117

POSTMASTER: If Undeliverable (Section 158 Postal Manual) Do Not Return

"The aeronautical and space activities of the United States shall be conducted so as to contribute . . . to the expansion of human knowledge of phenomena in the atmosphere and space. The Administration shall provide for the widest practicable and appropriate dissemination of information concerning its activities and the results thereof."

—NATIONAL AERONAUTICS AND SPACE ACT OF 1958

NASA SCIENTIFIC AND TECHNICAL PUBLICATIONS

TECHNICAL REPORTS: Scientific and technical information considered important, complete, and a lasting contribution to existing knowledge.

TECHNICAL NOTES: Information less broad in scope but nevertheless of importance as a contribution to existing knowledge.

TECHNICAL MEMORANDUMS: Information receiving limited distribution because of preliminary data, security classification, or other reasons. Also includes conference proceedings with either limited or unlimited distribution.

CONTRACTOR REPORTS: Scientific and technical information generated under a NASA contract or grant and considered an important contribution to existing knowledge.

TECHNICAL TRANSLATIONS: Information published in a foreign language considered to merit NASA distribution in English.

SPECIAL PUBLICATIONS: Information derived from or of value to NASA activities. Publications include final reports of major projects, monographs, data compilations, handbooks, sourcebooks, and special bibliographies.

TECHNOLOGY UTILIZATION PUBLICATIONS: Information on technology used by NASA that may be of particular interest in commercial and other non-aerospace applications. Publications include Tech Briefs, Technology Utilization Reports and Technology Surveys.

Details on the availability of these publications may be obtained from:

SCIENTIFIC AND TECHNICAL INFORMATION OFFICE

NATIONAL AERONAUTICS AND SPACE ADMINISTRATION

Washington, D.C. 20546